Article

Position Matters: Effect of Nitro Group in Chalcones on Biological Activities and Correlation via Molecular Docking

Alam Yair Hidalgo [1,2], Nancy Romero-Ceronio [1], Carlos Ernesto Lobato-García [1], Maribel Herrera-Ruiz [3], Romario Vázquez-Cancino [1], Omar Aristeo Peña-Morán [4], Miguel Ángel Vilchis-Reyes [1], Ammy Joana Gallegos-García [5], Eric Jaziel Medrano-Sánchez [1], Oswaldo Hernández-Abreu [1] and Abraham Gómez-Rivera [1,*]

1   División Académica de Ciencias Básicas, Universidad Juárez Autónoma de Tabasco, Carretera Cunduacán-Jalpa Km 1, Col. La Esperanza, Cunduacán 86690, Tabasco, Mexico; alam.yair.hidalgo@gmail.com (A.Y.H.); nrcdocencia@gmail.com (N.R.-C.); carloslobatogarcia@gmail.com (C.E.L.-G.); romavazquez197@gmail.com (R.V.-C.); mavilchisr@gmail.com (M.Á.V.-R.); ericsanz123@gmail.com (E.J.M.-S.); oswaldohernandezabreu@gmail.com (O.H.-A.)
2   Tecnológico Nacional de México-Instituto Tecnológico Superior de Comalcalco, Carretera Vecinal, Comalcalco-Paraiso Km 2, R/a Occidente 3ra Sección, Comalcalco 86650, Tabasco, Mexico
3   Centro de Investigación Biomédica del Sur, Instituto Mexicano del Seguro Social, Calle Rep. Argentina #1, Xochitepec 62780, Morelos, Mexico; cibis_herj@yahoo.com.mx
4   División de Ciencias de la Salud, Universidad de Quintana Roo, Av. Erick Paolo Martínez S/N, Esquina Av. 4 de Marzo, Chetumal C.P. 77039, Quintana Roo, Mexico; omar.moran@uqroo.edu.mx
5   División de Ciencias Básicas e Ingeniería, Universidad Popular de la Chontalpa-Carretera Cárdenas-Huimanguillo Km 2 S/N, Ranchería, Invitab Paso y Playa, Heroica Cárdenas 86556, Tabasco, Mexico; joana90102010@gmail.com
*   Correspondence: abgori@gmail.com

check for updates

Abstract: A series of nine nitro group-containing chalcones were synthesized to investigate their anti-inflammatory and vasorelaxant activities via in vivo, ex vivo, and in silico studies. The anti-inflammatory effects of the compounds were evaluated via a TPA-induced mouse ear edema model, and the vasorelaxant effects were evaluated via an isolated organ model in addition to molecular docking studies. The compounds with the highest anti-inflammatory activity were **2** (71.17 ± 1.66%), **5** (80.77 ± 2.82%), and **9** (61.08 ± 2.06%), where the nitro group is located at the ortho position in both rings, as confirmed by molecular docking with COX-1 and COX-2. The compounds with the highest vasorelaxant activity were **1** (81.16 ± 7.55%), lacking a nitro group, and **7** (81.94 ± 2.50%), where the nitro group is in the para position of the B ring; both of these compounds interact with the eNOS enzyme during molecular docking. These results indicate that the position of the nitro group in the chalcone plays an important role in these anti-inflammatory and vasorelaxant activities.

Keywords: chalcones; nitro group; anti-inflammatory activity; vasorelaxant activity; docking

1. Introduction

Inflammation is a natural process that is activated by a wide range of harmful conditions. In most cases, this process is beneficial, self-limiting, and quickly resolved [1]. However, inflammation can become chronic and has been associated with the etiology of several relevant clinical conditions, including cancer, arthritis, obesity, inflammatory bowel disease, and cardiovascular complications [2,3]. Traditionally, the treatment of chronic inflammation has included steroids and nonsteroidal anti-inflammatory drugs (NSAIDs) [4]. Both classes of drugs have side effects that range from mild to severe, affecting principally the gastrointestinal tract and cardiovascular system or generating allergic reactions [5]. For this reason, the development of new substances with anti-inflammatory potential is highly important [6].

Flavonoids are a family of compounds that have demonstrated anti-inflammatory activity. Among them, chalcones have garnered considerable interest due to their wide range of pharmacological properties, including anti-inflammatory, vasorelaxant, antibacterial, analgesic, antiplatelet, anticholinergic, antimalarial, antiviral, anticancer, antileishmanial, antioxidant, and antispasmodic effects, among others [7–12]. The structure of chalcones is composed of two benzene rings (rings A and B) linked by a three-carbon α, β-unsaturated ketone (enone). This last moiety is highly electrophilic, with a conjugated double bond and a completely delocalized π-electron distribution on the aromatic rings [13,14], a property that can be modulated by substituting aromatic rings A or B with different functional groups [15,16]. This has resulted in the synthesis of novel chalcones, which have been studied for their physical, chemical, and biological properties [17]. The efficacy, safety, and therapeutic effects of these chalcones have been analyzed [18,19], and it has been demonstrated that they serve as efficacious models for the development of novel therapeutic agents [20]. It has been previously reported that chalcones containing a nitro group possess anti-inflammatory effects. The mechanism by which these compounds exert their biological effects is attributed to their ability to inhibit a number of enzymes associated with inflammation, including cyclooxygenase (COX) and lipoxygenase (LOX) [21]. Furthermore, both these enzymes are implicated in a range of other diseases and conditions that represent significant global health burdens, including cardiovascular disease, cancer, diabetes mellitus, asthma, chronic obstructive pulmonary disease, obesity, and arthritis [22–24].

In addition, some chalcones can also induce vasorelaxation, a phenomenon related to the nitric oxide (NO) and estrogen receptor α (Erα) pathways [25]. This is crucial in the context of cardiovascular diseases, which affect a significant portion of the adult population worldwide [26]. Many investigations into the mechanisms of action by which chalcones exert anti-inflammatory and vasorelaxant effects via molecular docking methods have revealed a plethora of interactions related to their calcium channel blocking activity and the inhibition of interleukin-6 (IL-6) and tumor necrosis factor-alpha (TNF-α) induced by lipopolysaccharide (LPS) [27,28].

Current pharmaceuticals that contain the nitro group in their structure [29], exemplified by the antibiotic metronidazole [30] and the anticancer drug venetoclax [31], are known to exert their pharmacological effects primarily through this moiety. Therefore, the presence of this functional group is of paramount importance given the polar and electronic properties that enable them to interact with specific targets that play a pivotal role in the pathogenesis of numerous diseases [32].

The objective of this study was to evaluate the anti-inflammatory and vasorelaxant properties of a series of nitro group-containing chalcones previously synthesized by our research group [33–36] through in vivo, ex vivo, and in silico investigations (Figure 1). The compounds that exhibited the most pronounced pharmacological activity were subsequently evaluated in terms of their dose–response and concentration–response relationships, as well as through molecular docking studies involving the relevant targets for anti-inflammatory and vasorelaxant effects, namely the COX-1, COX-2, and eNOS enzymes.
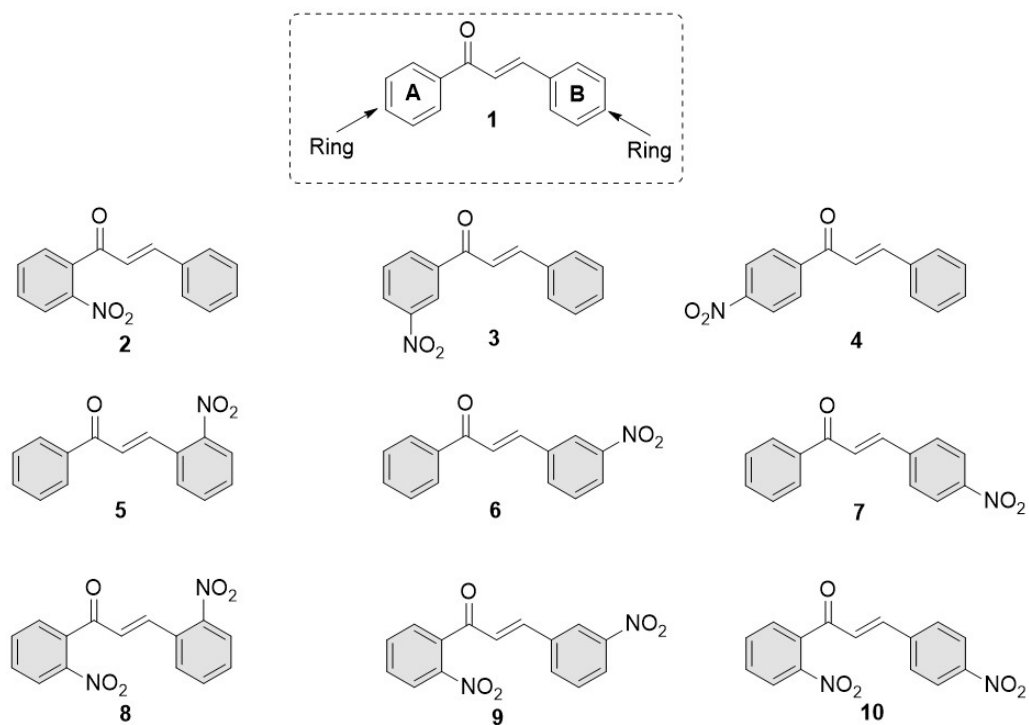
Figure 1. Previously synthesized chalcones were evaluated for their anti-inflammatory and vasorelaxant activities [33–36].

2. Materials and Methods

2.1. Synthesis

Compounds **1**–**10** were synthesized as previously reported by our research group at the División Académica de Ciencias Básicas of the Universidad Juárez Autónoma de Tabasco (UJAT). The physicochemical and spectroscopic data have been previously published [33–36].

2.1.1. General Procedure for the Synthesis of Chalcone **1**

Benzaldehyde (0.81 mmol) was added to ethanol (8 mL) and stirred continuously at 0 °C. Acetophenone (0.81 mmol) and a 1 M NaOH solution (4 mL, 0.81 mmol) were then added dropwise. The mixture was stirred vigorously until it reached 28 ± 2 °C. The reaction progress was monitored by thin-layer chromatography (TLC) using silica gel and an ethyl acetate/hexane mixture (20:80), visualized under UV light or with potassium permanganate ($KMnO_4$). The resulting solid was filtered, washed with distilled water, and recrystallized from a dichloromethane/hexane [33].

2.1.2. General Procedure for the Synthesis of Nitrochalcones **2**–**4**

Sodium hydroxide (6.7 mmol) was dissolved in water (6 mL) and cooled to 0 °C in an ice bath. Ethanol (10 mL) was slowly added, and the mixture was allowed to warm to room temperature. Acetophenone (10 mmol) was gradually added, followed by the slow addition of benzaldehyde (10 mmol). The reaction was stirred at room temperature for 2 h and then cooled to 0 °C for 24 h. The precipitate was filtered, washed with cold water, and recrystallized from a dichloromethane/ethanol mixture. The crystals were dried at 70 °C [34].

2.1.3. General Procedure for the Synthesis of Nitrochalcones **5**–**7**

Nitrobenzaldehyde (1 mmol) was dissolved in ethanol (3 mL) and stirred at 0 °C in an ice bath. Aqueous sodium hydroxide (0.1 equivalents, 0.05 M) and acetophenone (1 mmol) were simultaneously added. The reaction mixture was stirred at room temperature for 3 h

and then cooled to 0 °C for 24 h. The resulting solid was filtered, washed with cold water, and purified by recrystallisation using a dichloromethane/hexane solvent pair [35].

2.1.4. General Procedure for the Synthesis of Nitrochalcones **8**–**10**

2-Nitroacetophenone (10 mmol) was dissolved in ethanol (10 mL) and placed in an ice–salt bath. Sodium hydroxide (6 mL, 1.0 M) was added, and the mixture was stirred for 15 min. Nitrobenzaldehyde (10 mmol) was then added, and the reaction was stirred at room temperature for 3 h. The reaction progress was monitored by TLC. The solid product was filtered, washed with water, and recrystallized using a dichloromethane/n-hexane solvent pair [36].

2.2. *Characterization of Compounds* **1**–**10** *[34–36]*

(*E*)-1,3-diphenyl-prop-2-en-1-one (**1**) yield: 85%; yellow solid; m.p. 53 °C. ^{1}H NMR spectrum (600 MHz, CDCl$_3$) δ (ppm): 8.02 (d, J = 6.0, 1.5 Hz, 1H), 7.82 (d, J = 15.6 Hz, 1H), 7.64–7.61 (m, 1H), 7.56 (t, J = 7.2, 1.5 Hz, 1H), 7.52 (d, J = 15.6 Hz, 1H), 7.48 (t, J = 7.2, 6.0 Hz, 1H), 7.43–7.38 (m, 2H). ^{13}C NMR spectrum (150 MHz, CDCl$_3$) δ (ppm): 122.6, 129.0, 129.1, 129.2, 129.5, 131.1, 133.4, 135.4, 138.7, 145.4, 191.1.

(*E*)-1-(2′-nitrophenyl)-3-phenylprop-2-en-1-one (**2**) yield: 72.2%; white solid; m.p. 136–138 °C. ^{1}H NMR spectrum (400 MHz, CDCl$_3$) δ (ppm): 8.16 (d, J = 8 Hz, 1H), 7.76 (t, J = 7.4 Hz, 1H), 7.65 (t, J = 7.6 Hz, 1H), 7.49 (m, 3H), 7.37 (m, 3H), 7.23 (d, J = 16.3 Hz, 1H), 7.16 (d, J = 16.3 Hz, 1H). ^{13}C NMR spectrum (100 MHz, CDCl$_3$) δ (ppm): 192.9, 146.6, 146.3, 136.1, 133.9, 133.8, 131.0, 130.5, 128.9, 128.7, 128.1, 126.1, 124.4.

(E)-1-(3′-nitrophenyl)-3-phenylprop-2-en-1-one (**3**) yield: brown solid (73.2%); m.p. 135–136 °C. ^{1}H NMR spectrum (400 MHz, CDCl$_3$) δ (ppm): 8.82 (t, J = 1.8 Hz, 1H), 8.43 (ddd, J = 1.0, 1.8, 8.0 Hz, 1H), 8.35 (d, J = 7.8 Hz, 1H), 7.88 (d, J = 15.6 Hz, 1H), 7.72 (t, J = 7.8 Hz, 1H), 7.68–7.66 (m, 2H), 7.54 (d, J = 15.6 Hz, 1H), 7.46–7.44 (m, 3H). ^{13}C NMR spectrum (100 MHz, CDCl$_3$) δ (ppm): 187.9, 148.3, 146.7, 139.4, 134.2, 134.0, 131.1, 129.9, 129.0, 128.7, 127.0, 123.2, 120.5.

(*E*)-1-(4′-nitrophenyl)-3-phenylprop-2-en-1-one (**4**) yield: yellow solid (72.1%); m.p. 156–158 °C. ^{1}H NMR spectrum (400 MHz, CDCl$_3$) δ (ppm): 8.34 (d, J = 8.9 Hz, 2H), 8.14 (d, J = 8.9 Hz, 2H), 7.84 (d, J = 15.7 Hz, 1H), 7.67–7.65 (m, 3H), 7.49 (d, J = 15.7 Hz, 1H), 7.45 (dd, J = 1.2, 5.1 Hz, 2H). ^{13}C NMR spectrum (100 MHz, CDCl$_3$) δ (ppm): 188.9, 149.9, 146.7, 142.9, 134.2, 131.2, 129.3, 129.0, 128.6, 123.8, 121.2.

(*E*)-3-(2-nitrophenyl)-1-phenylprop-2-en-1-one (**5**) yield: 90%; yellow solid; m.p. 115–116 °C. ^{1}H NMR spectrum (400 MHz, CDCl$_3$) δ (ppm): 7.34 (d, J = 15.6 Hz, 1H), 7.51 (m, 2H), 7.58 (m, 2H), 7.72 (m, 2H), 8.01 (m, 2H), 8.04 (dd, J = 5.64, 1.2 Hz, 1H), 8.13 (d, J = 15.6 Hz, 1H). ^{13}C NMR spectrum (100 MHz, CDCl$_3$) δ (ppm): 124.8, 127.0, 128.6, 128.6, 129.1, 130.2, 131.1, 133.0, 133.5, 137.2, 140.0, 148.3, 190.2.

(E)-3-(3-nitrophenyl)-1-phenylprop-2-en-1-one (**6**) yield: 94%; white solid; m.p. 132–134 °C. ^{1}H NMR spectrum (400 MHz, CDCl$_3$) δ (ppm): 7.56 (m, 4H), 7.67 (d, J = 16 Hz, 1H), 7.83 (d, J = 16 Hz, 1H), 7.93 (d, J = 7.8 Hz, 1H), 8.05 (m, 2H), 8.25 (dd, J = 8.1, 2.1 Hz, 1H), 8.50 (dd, J = 2.1, 1.8 Hz, 1H). ^{13}C NMR spectrum (100 MHz, CDCl$_3$) δ (ppm): 122.2, 124.4, 124.5, 128.5, 128.7, 129.9, 133.2, 134.2, 136.5, 137.4, 141.5, 148.5, 189.5.

(E)-3-(4-nitrophenyl)-1-phenylprop-2-en-1-one (**7**) yield: 90%; yellow solid; m.p. 156–158 °C. ^{1}H NMR spectrum (400 MHz, CDCl$_3$) δ (ppm): 7.53 (dt, J = 7.6, 1.5 Hz, 2H), 7.61 (d, J = 7.6 Hz, 1H), 7.65 (d, J = 15.54 Hz, 1H), 7.78 (d, J = 8.7 Hz, 2H), 7.81 (d, J = 15.54 Hz, 1H), 8.04 (dd, J = 7.8, 1.5 Hz, 2H,), 8.26 (d, J = 8.7 Hz, 2H). ^{13}C NMR spectrum (100 MHz, CDCl$_3$) δ (ppm): 124.1, 125.5, 128.5, 128.7, 128.8, 133.3, 137.4, 140.9, 141.4, 148.4, 189.5.

(*E*)-1,3-bis(2-nitrophenyl)prop-2-en-1-one (**8**) yield: 42%; white solid; m.p. 140–142 °C. ^{1}H NMR spectrum (600 MHz, DMSO-*d*^{6}) δ (ppm): 8.25 (d, J = 8.1 Hz, 1H), 8.08 (d, J = 8.1 Hz, 1H), 8.01 (d, J = 7.7 Hz, 1H), 7.95 (t, J = 7.3 Hz, 1H), 7.85–7.80 (m, 2H), 7.75 (d, J = 7.4 Hz, 1H), 7.70 (t, J = 7.9 Hz, 1H), 7.66 (d, J = 16.1 Hz, 1H), 7.24 (d, J = 16.1 Hz, 1H). ^{13}C NMR

spectrum (150 MHz, DMSO-d^6, DEPTQ) δ (ppm): 192.6, 148.8, 146.9, 141.6, 135.3, 135.1, 134.4, 132.2, 131.8, 130.0, 129.8, 129.7, 129.6, 125.3, 125.1.

(*E*)-1-(2-nitrophenyl)-3-(3-nitrophenyl)prop-2-en-1-one (**9**) yield: 90%; white solid; m.p. 145–147 °C. ^{1}H NMR spectrum (600 MHz, DMSO-d^6) δ (ppm): 8.58 (s, 1H), 8.25–8.22 (m, 3H), 7.92 (t, J = 7.4 Hz, 1H), 7.83 (t, J = 7.7 Hz, 1H), 7.74 (d, J = 7.4 Hz, 1H), 7.70 (t, J = 7.9 Hz, 1H), 7.57 (d, J = 16.3 Hz, 1H), 7.51 (d, J = 16.3 Hz, 1H). ^{13}C NMR spectrum (150 MHz, DMSO-d^6, DEPTQ) δ (ppm): 192.6, 148.7, 147.0, 143.6, 136.3, 135.6, 135.0, 134.9, 132.0, 130.8, 129.5, 128.6, 125.4, 125.0, 123.9.

(*E*)-1-(2-nitrophenyl)-3-(4-nitrophenyl)prop-2-en-1-one (**10**) yield: 81%; yellow solid; m.p. 175–177 °C. ^{1}H NMR spectrum (600 MHz, DMSO-d^6) δ (ppm): 8.24–8.22 (m, 3H), 8.01 (m. 2H), 7.93 (t, J = 7.4 Hz, 1H), 7.83 (t, J = 7.7 Hz, 1H), 7.76 (d, J = 7.4 Hz, 1H), 7.53 (d, J = 16.2 Hz, 1H), 7.48 (d, J = 16.2 Hz, 1H). ^{13}C NMR spectrum (150 MHz, DMSO-d^6, DEPTQ) δ (ppm): 192.5, 148.7, 147.0, 143.1, 140.8, 135.4, 135.0, 132.1, 130.3, 129.7, 129.5, 125.1, 124.3.

2.3. Animals

The experiments on anti-inflammatory activity were conducted using male ICR mice weighing 25–30 g sourced from Envigo RMS, S.A. de C.V., kept in the bioterium of the Centro de Investigación Biomédica del Sur (CIBIS-IMSS). For vasorelaxant activity, male Wistar rats (250–300 g) were obtained from the Unidad de Producción, Cuidado y Experimentación Animal (UPCEA), which is affiliated with the División Académica de Ciencias de la Salud (UJAT). In both cases, the animals were maintained under a 12 h light–dark cycle at a constant temperature (23–25 °C) with free access to food and water, and were treated according to the Mexican Federal Regulations for the Care and Use of Laboratory Animals, NOM-062-ZOO-1999 Guidelines [37], as well as the international ethical guidelines for the care and use of laboratory animals [38]. The animal studies were approved by the Ethics Committee of the Instituto Mexicano del Seguro Social (R-2020-1702-008) and by the Institutional Commission on Research Ethics (CIEI-UJAT-0927).

2.4. Anti-Inflammatory Activity

The number of animals utilized (*n* = 5 for each treatment) and the intensity of the noxious stimuli employed were the minimum necessary to demonstrate the consistent effects of the pharmacological treatments.

The induction of auricular inflammation was performed in accordance with previously described methods [39]. The dose evaluated for the compounds was 1.0 mg/ear. The control group was treated with acetone as a vehicle, and 1.0 mg/ear indomethacin (**Indo**, Sigma–Aldrich, Toluca, Mexico) was used as an anti-inflammatory positive control. All treatments were prepared by dissolving the appropriate quantity of the active ingredient in acetone and applying the solution topically to both ears immediately after the solution of 12-O-tetradecanoylphorbol-13-acetate (TPA; Sigma–Aldrich, Toluca, Mexico), which was used as an inflammatory agent. Six hours after the administration of TPA, the animals were euthanized via cervical dislocation. Circular sections 6 mm in diameter were excised from both the treated (t) and nontreated (nt) ears and weighed to determine the extent of inflammation. The percentage of inhibition was calculated via the following equation:

$$\text{\% inhibition} = [\text{Dw control} - \text{Dw treated}/\text{Dw control}] \times [100],$$

where Dw = wt − wnt. In this expression, wt represents the weight of the treated ear section, and wnt denotes the weight of the untreated ear section.

2.5. Vasorelaxant Activity

The animals were anesthetized via the injection of sodium pentobarbital (60 mg/kg, intraperitoneally) and subsequently euthanized via cervical dislocation. Aortic rings (3–5 mm) were cleaned of connective tissue and fat (in some rings, the endothelium was removed). Tissues were extracted under optimal tension (3 g) in Krebs solution (composition, mM: NaCl, 118; KCl, 4.7; CaCl$_2$, 2.5; MgSO$_4$, 1.2; KH$_2$PO$_4$, 1.2; NaHCO$_3$,

25.0; EDTA, 0.026; and glucose, 11.1, pH 7.4) at 37 °C and oxygenated (O_2/CO_2 ratio, 19:1) in a thermostatically controlled water bath. The solution was maintained at 37 °C and oxygenated with a gas mixture comprising 19% oxygen and 1% carbon dioxide. Isometric tension was recorded via TSD125 C force transducers, which were used in conjunction with a DA100C amplifier (Astromed®, West Warwick, RI, USA) and connected to an MP160 analyzer (Biopac® Instruments, Santa Barbara, CA, USA), as previously described [40]. Following the equilibrium period, denuded and intact aortic rings were precontracted with noradrenaline bitartrate (NA; Sigma–Aldrich Co., St. Louis, MO, USA) at a concentration of 0.1 µM, and subsequently washed every 30 min. The absence of a relaxation response to 1 µM carbamylcholine chloride (carbachol, Sigma–Aldrich Co., St. Louis, MO, USA) confirmed the presence of the endothelium. Under these conditions, the relaxant effect and vascular mode of action were determined.

The aortic rings, with or without endothelium, were contracted with NA (0.1 µM). After 15 min, once a plateau was reached, the compounds (1–10; 0.1–10 µg/mL), carbachol (1×10^{-4}–10 µM), and nitrendipine (Sigma–Aldrich Co., St. Louis, MO, USA) at concentrations ranging from 1×10^{-4} to 10 µM or vehicle (0.1% DMSO) were added to the bath chamber in a cumulative manner. Muscular tone was calculated both before and after the addition of increasing concentrations. The data were analyzed via the AcqKnowledge 5.0 software. To elucidate the endothelial signaling pathway engaged by chalcones (muscarinic receptors, eNOS, or COX-1), aortic rings with endothelium were treated with **Indo** (Sigma–Aldrich Co., St. Louis, MO, USA) and N-nitro-L-arginine methyl ester (L-NAME, Sigma–Aldrich Co., St. Louis, MO, USA) at a concentration of 10 µM, or with atropine (Sigma–Aldrich Co., St. Louis, MO, USA) at a concentration of 1 µM, for 15 min before contracting the arterial rings with NA (0.1 µM). The most active compounds (**1** and **7**) were subsequently added at cumulative concentrations (0.1–10 µg/mL). Muscle tone was calculated in the presence and absence of **Indo**, L-NAME, or atropine [41].

2.6. Molecular Docking Calculations

The COX-1 model (pdb: 3kk6) [42] was obtained from the Protein Data Bank (PDB) repository with a resolution of 2.75 Å. The COX-1 model was found to contain celecoxib (CEL) as a ligand. The grid was positioned at the coordinates of the CEL site, which were determined to be X = −32.591, Y = 42.338, and Z = −6.333. The COX-2 model (PDB: 3ln1) [43] cocrystallized with CEL was downloaded from the same repository with 2.40 Å resolution; the grid was located at the coordinates X = 30.060, Y = −21.639, and Z = −16.698.

For both models, the grid had dimensions of 45 points (16.87 Å) per side, with a spacing of 0.375 Å. The alignment of COX-1 and COX-2 was performed with the Align tool from the UniProt database, and the identity and similarity percentages were calculated manually. To analyze the selectivity of compounds between COX-1 and COX-2, the affinity constant (Ki) was obtained via the Gibbs free energy equation. The selectivity index was defined as the ratio of the Ki values for COX-1 and COX-2. A selectivity index of 10 or greater was deemed a sufficient indicator of selectivity.

The eNOS model (PDB: 4d1o) [44] was obtained from the PDB repository with a resolution of 1.82 Å. This model contained 5,6,7,8-tetrahydrobiopterin (H4B) as a ligand, and the grid (18.0 Å per side) was positioned at the H4B site at the following coordinates: X = 17.422, Y = 234.059, and Z = 22.246.

The models of chalcones **1–10** were optimized via a total energy minimization force field of MMFF94 (Avogadro software v1.1.1) [45]. The compounds were docked into the active sites of COX-1, COX-2, and eNOS via AutoDock Tools and the AutoDock Vina executable [46,47], with the precise locations corresponding to those observed for CEL or H4B in the crystallized structures. In the preceding phase, polar hydrogen atoms were incorporated into the biomacromolecule models, and Kollman charges (AMBERs) were assigned. A total of 100 poses were obtained for each compound **1–10**, with **Indo**, CEL, and H4B serving as the control compounds. The most populated cluster was subjected to analysis, and the average energy pose was visualized with the Discovery Studio v3.5

software [48]. The protocol was validated by docking the cocrystallized ligands into their respective binding sites, with a root-mean-square deviation (RMSD) of less than 2.0 Å considered for model validation.

2.7. Statistical Analysis

The data reported are presented as the mean $\pm$ standard error of the mean (SEM). The statistical significance of the results was determined via analysis of variance (ANOVA) with a confidence level of 95% (* $p \leq 0.05$), followed by the one-tailed Dunnett test in comparison with the control (**Indo**) and Tukey's test. The results of the vasorelaxant activity are expressed as the mean of five experiments $\pm$ standard error of the mean (SEM) concentration–response curves. The statistical significance ($p \leq 0.05$) of differences between means was assessed by ANOVA, followed by Tukey's test.

All the statistical analyses were conducted via IBM SPSS Statistics version 23.0 software. The median effective dose (ED50) and median effective concentration (EC50) were calculated via linear regression via GraphPad Prism 8.0.2 (San Diego, CA, USA).

3. Results

3.1. Anti-Inflammatory Evaluation

The anti-inflammatory efficacy of chalcone 1 and the set of chalcones containing nitro groups (compounds **2–10**) was evaluated in a TPA-induced mouse ear model. All compounds demonstrated anti-inflammatory activity at a dose of 1 mg/ear (Figure 2).

The percentage inhibition of chalcone **1** was 31.75 $\pm$ 1.49%, and for the nitro group-containing chalcones **2–10**, the percentages of inhibition were 71.17 $\pm$ 1.66%, 18.32 $\pm$ 1.53%, 58.25 $\pm$ 1.97%, 80.77 $\pm$ 2.82%, 52.62 $\pm$ 1.37%, 30.09 $\pm$ 0.67%, 16.82 $\pm$ 0.95%, 61.08 $\pm$ 2.06%, and 13.22 $\pm$ 2.08%, respectively. For the positive control (**Indo**), the observed percentage inhibition was 71.48 $\pm$ 1.62%.

Compounds **2** and **5**, which both possess a nitro group at the ortho position (on the A and B rings, respectively), exhibited the highest percentage of inhibition. Specifically, chalcone **5** exhibited notable distinctions and demonstrated the most pronounced effect in comparison to the other compounds under examination and to **Indo**. Moreover, the effects of compound **2** were statistically comparable to those of the reference drug. Furthermore, compounds **4** and **9** exhibited notable activity, with no significant differences between them. Notably, compound **4** has a nitro group at the para position (on ring B), whereas compound **9**, which has a nitro group at the ortho and meta positions (ring A and ring B, respectively), is the only disubstituted compound that demonstrated substantial anti-inflammatory activity. Similarly, the statistical analysis of the remaining compounds in comparison with **Indo** revealed significant differences at the $p \leq 0.05$ level. Finally, some nitrochalcones were not significantly different; consequently, they had similar effects: chalcones **1** and **7**; chalcones **3**, **8**, and **10**; and chalcones **4** and **6**.

The most active compounds (**2**, **5**, and **9**) were evaluated at various doses (0.125, 0.25, 0.5, 1.0, and 2.0 mg/ear) to obtain their dose–response anti-inflammatory effects. In the case of Indo, it was only at the 1.0 mg/ear dose that the doses of the compounds were compared. At all the tested doses, edema was reduced in a dose-dependent manner (Figure 3). The inhibition percentages for compound **2** were as follows: 41.60 $\pm$ 1.55%, 47.50 $\pm$ 1.35%, 54.83 $\pm$ 0.95%, 70.53 $\pm$ 1.43%, and 62.75 $\pm$ 1.71%. The inhibition percentages for compound **5** were 32.61 $\pm$ 1.62%, 32.35 $\pm$ 2.10%, 38.88 $\pm$ 3.10%, 80.43 $\pm$ 2.21%, and 68.54 $\pm$ 2.45%, whereas for compound **9**, the inhibition percentages were 25.42 $\pm$ 1.22%, 41.93 $\pm$ 2.25%, 48.1 $\pm$ 2.29%, 61.39 $\pm$ 1.63%, and 50.48 $\pm$ 1.66%, respectively. Notably, the doses of 1 and 2 mg/ear of compounds **2** and **5** did not significantly differ from that of **Indo** at 1 mg/ear. Conversely, the other doses demonstrated significant differences with respect to the reference drug (Figure 3).

From the dose–response curves of each of the compounds, the mean response dose (ED50) was obtained: for compound **2**, the ED50 was 1.07 μM; for **5**, it was 1.64 μM; and for **9**, it was 1.67 μM. Compound **2** had the lowest ED50 and was significantly different

from the other two compounds (Figure 3). Furthermore, a comparison of the ED50 values of each compound revealed that **2** was 1.57-fold and 1.84-fold more potent than **5** and **9**, respectively.

3.2. Vasorelaxant Activity Evaluation

The pharmacological parameters of the compounds evaluated and their controls with endothelium (E+) and without endothelium (E−) are presented in Table 1. The nitrochalcones demonstrated a partially endothelium-dependent and concentration-dependent vasorelaxant effect. Compounds **1** and **7** presented higher E_{max} values than did the positive control, prompting an investigation into their mechanism of action.

The chalcone that demonstrated the most pronounced vasorelaxant effect was **1**, which lacks a nitro group and exhibited a relaxation of 81.16 ± 7.55% in the presence of endothelium and 45.64 ± 6.65% in its absence. The statistical analysis of both experiments conducted on compound **1** revealed significant differences between them. With respect to the nitro group-containing chalcones, compound **7** presented the most pronounced vasorelaxant activity, with an E_{max} value of 81.94 ± 2.50% in the presence of endothelium and 8.84 ± 3.45% in its absence. The statistical analysis of the experiments conducted on compound **7** revealed significant differences.
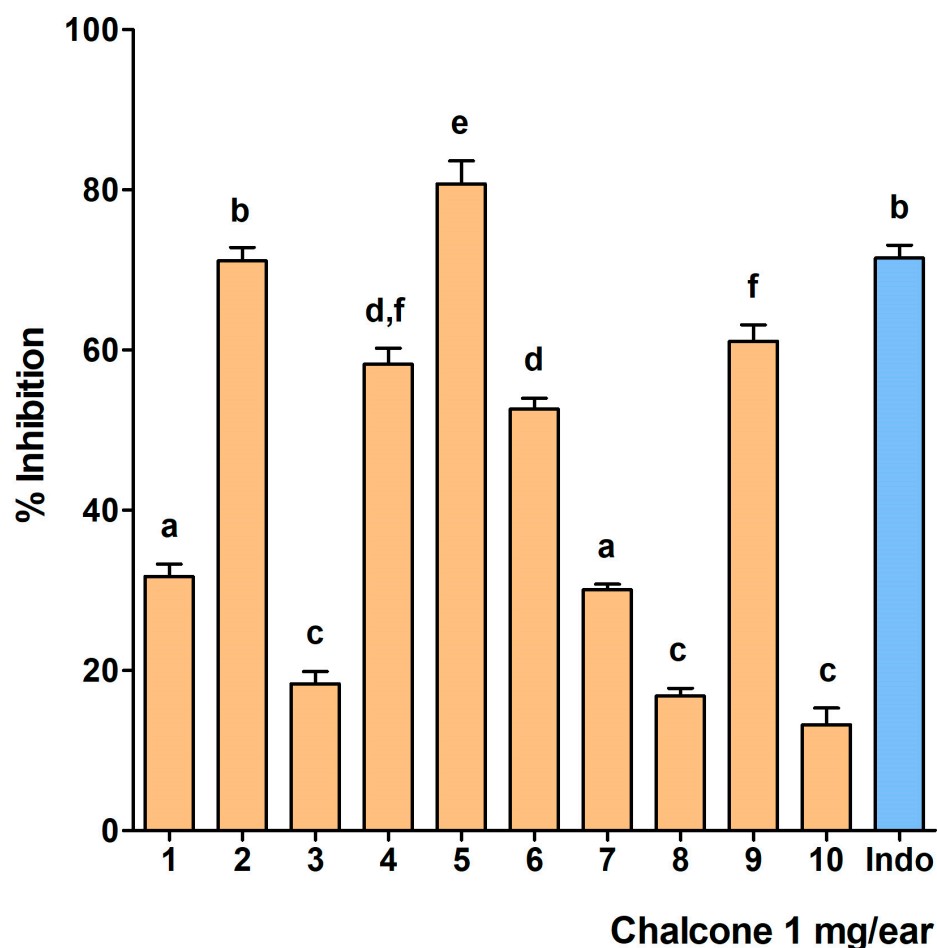
Figure 2. Comparison of the inhibitory effects of chalcones **1–10** on inflammation in the TPA-induced mouse ear edema model. The data are reported as the mean ± standard error (n = 5 for each treatment). The statistical significance of the observed differences was determined by analysis of variance (ANOVA) followed by Tukey's test. Bars with the same letter (a–f) indicate that the groups do not differ significantly at $p \leq 0.05$.
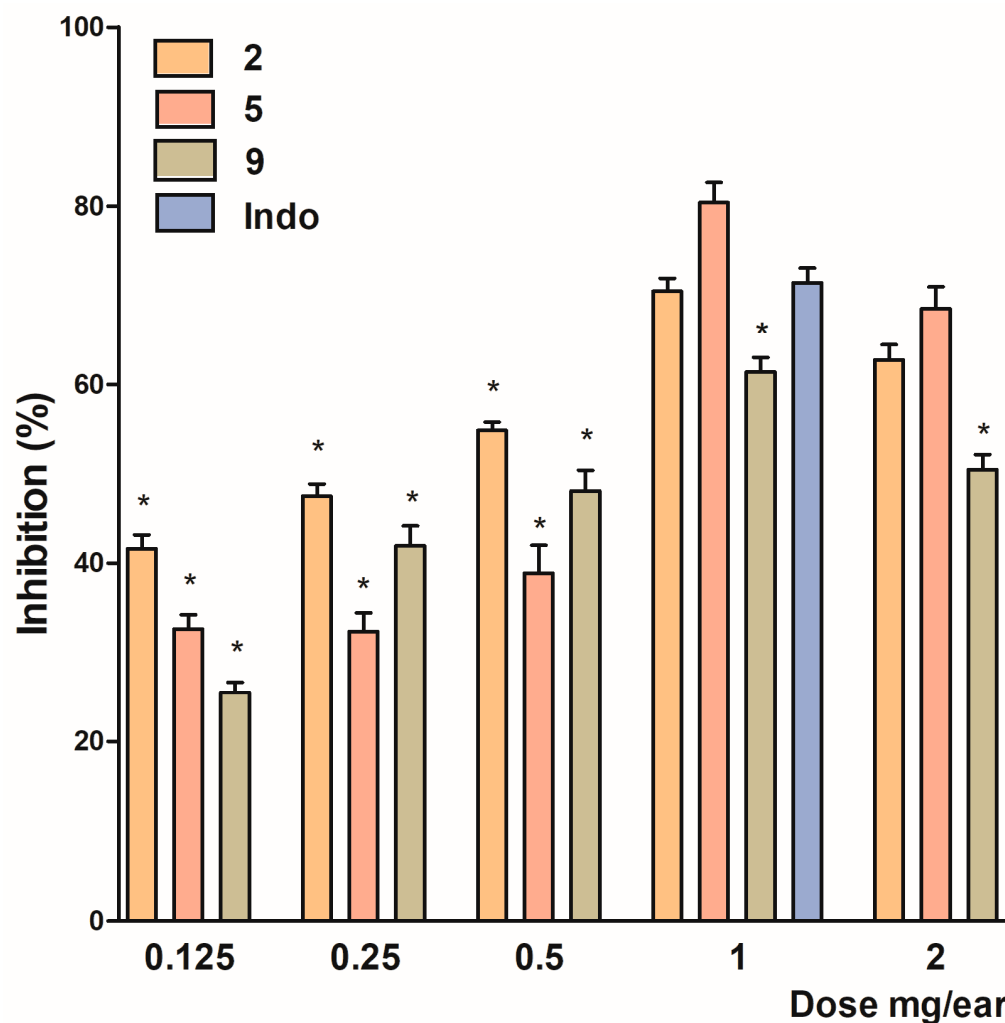
Figure 3. Anti-inflammatory effects of compounds **2**, **5** and **9** at different doses and Indo at a single dose. The values are reported as the means $\pm$ standard errors (n = 5 for each treatment). Statistical differences were determined by analysis of variance (ANOVA), followed by Dunnet's test. * $p \leq 0.05$ vs. **Indo**.

Table 1. Vasorelaxant effect induced by compounds **1–10** with contractions produced by NA (0.1 μM).

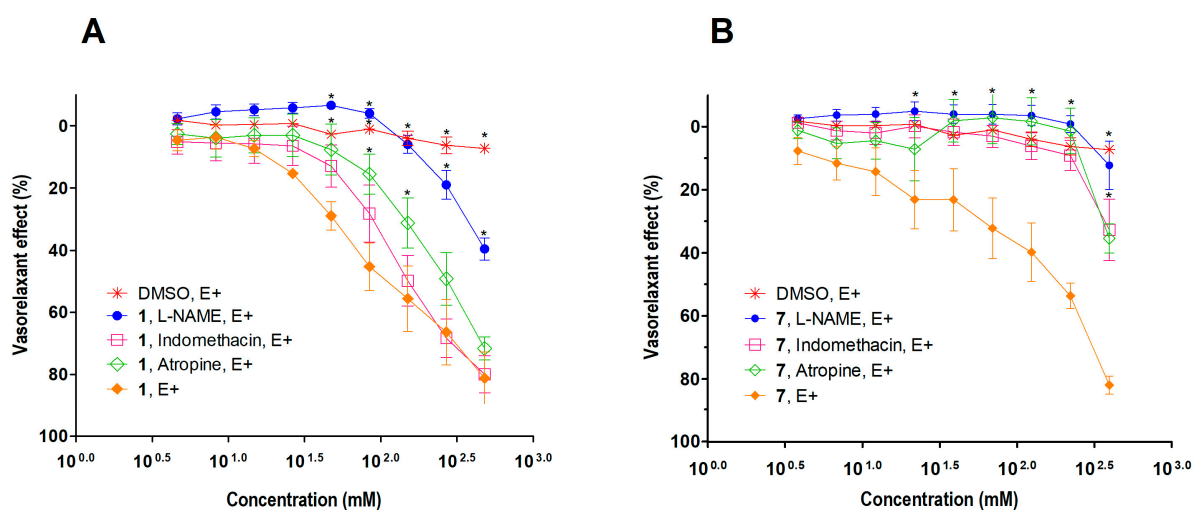| Compound	With Endothelium (E+)		Without Endothelium (E−)	
	E_{max}	EC_{50} (μM)	E_{max}	EC_{50} (μM)
1	81.16 ± 7.55	159.01	45.64 ± 6.65 **	ND
2	57.04 ± 9.54 *	144.32	26.45 ± 5.64 **	ND
3	66.23 ± 13.35 *	364.17	12.65 ± 2.09 **	ND
4	43.25 ± 2.91 *	ND	27.52 ± 6.50 **	ND
5	39.23 ± 5.10 *	ND	23.64 ± 3.24 **	ND
6	-7.94 ± 11.84 *	ND	16.16 ± 3.56 **	ND
7	81.94 ± 2.50	381.64	8.84 ± 3.45 **	ND
8	47.24 ± 1.75 *	ND	53.42 ± 20.45 **	197.60
9	45.00 ± 17.35 *	ND	13.86 ± 1.85 **	ND
10	40.75 ± 7.27 *	ND	28.92 ± 1.97 **	ND
Carbachol	76.72 ± 7.88	358.64	---	---
Nitrendipine	---	---	90.29 ± 2.15	354.28

ND = not determined. E+ (* $p \leq 0.05$ carbachol). E− (** $p \leq 0.05$ nitrendipine).

In the experiments with endothelium present, compounds **1** and **7** presented the highest percentages of E_{max}, which did not significantly differ between them or with carbachol,

indicating a similar efficacy. However, compound 1 is more potent than compound **7** and carbachol, since it presents a lower EC50.

In the experiments without endothelium, compounds **1** and **8** had the highest percentages of E_{max}, which did not significantly differ between them but did differ from nitrendipine. Additionally, the IC50 of **8** was significantly different from that of nitrendipine.

Based on the vasorelaxant effect with and without endothelium, experiments were proposed to determine the mechanism of action because each type of cell (muscle and endothelial) has different relaxing factors. The most pronounced vasorelaxant effect was observed with compounds **1** and **7**, which prompted an investigation into potential pathways through which this activity was achieved. To this end, the compounds were evaluated in the presence of L-NAME (a nonspecific nitric oxide synthase inhibitor), **Indo** (a nonspecific COX inhibitor), and atropine (a cholinergic muscarinic receptor antagonist) (Figure 4).

Figure 4. Vasorelaxant effects of compounds **1** (**A**) and **7** (**B**) in the presence of L-NAME, **Indo**, and atropine on NA (0.1 μM)-induced contraction in aortic rings with endothelium. The data are presented as the means ± standard errors (n = 5 for each treatment). The statistical significance was determined by analysis of variance (ANOVA), followed by Tukey's test. A value of * $p \leq 0.05$ was considered statistically significant.

The vasorelaxant effect of compound **1** in aortic rings with E+ was observed to be $E_{max} = 81.16 \pm 7.55\%$. However, in the presence of L-NAME, the effect was reduced to $E = 39.59 \pm 3.18\%$. In tests with **Indo** and atropine, the response of the aortic rings with E+ was not significantly modified. In contrast, compound **7** demonstrated a right-shifted vasorelaxation effect in the presence of L-NAME, **Indo**, or atropine, with a corresponding decrease in its E value. Specifically, the E value decreased to $12.24 \pm 6.89\%$, $30.70 \pm 15.69\%$, and $35.39 \pm 4.10\%$, respectively.

3.3. Molecular Docking

Molecular docking calculations were implemented with crystallographic complexes obtained from the Protein Data Bank (PDB) database. With respect to anti-inflammatory activity, a molecular docking study was conducted with compounds **1**, **2**, **5**, and **9** in complex with the COX-1 protein (PDB: 3kk6) [42] and COX-2 (PDB: 3ln1) [43], and for vasorelaxant activities, with compounds **1** and **7** via the eNOS protein (PDB: 4d1o) [44].

3.3.1. Cyclooxygenase-1

The molecular docking results of compounds **1**, **2**, **5**, and **9** with COX-1 demonstrated an affinity energy range of −8.0−−7.5 kcal/mol, and the following interactions were observed: the carbonyls of compounds **1**, **2**, and **5** formed carbon hydrogen–hydrogen bonds with Ser[353], whereas the carbonyl group of compound **9** similarly interacted with

Ser[530]. The benzene ring A of compounds **1**, **2**, and **5** interacted with Leu[531] via a π–alkyl interaction, whereas ring B of these same compounds exhibited π–sigma interactions with Leu[352] and stacked amide–π-type interactions with Gly[526]. Similarly, Ala[527] interacted with the A and B rings of compounds **1**, **2**, and **5** via π–alkyl bonds. The presence of the nitro group in the ortho position of the A-ring of compound **2** resulted in the interaction of one of the oxygens of the nitro group with Arg[120] through conventional hydrogen bonding. Additionally, this ring exhibited further π–alkyl interactions with the amino acids Val[349], Leu[359], and Val[116], and π–sulfide interactions with Met[113]. In the ortho position of ring B of compound **5**, the nitro group engaged in a carbon–hydrogen bond with Ala[527]. Compound **9**, which is substituted with a nitro group at both the ortho position of ring A and the meta position of ring B, demonstrated interactions between ring A and Leu[352] of the π–sigma type, and with Gly[526] of the stacked amide–π type. In ring B, the π–sigma interactions were with Leu[531] and Val[349], whereas with Ala[527], they were of the π–alkyl type. For the nitro groups, only the one in ring B interacted with amino acid Arg[120] via conventional hydrogen bonding (Figure 5).
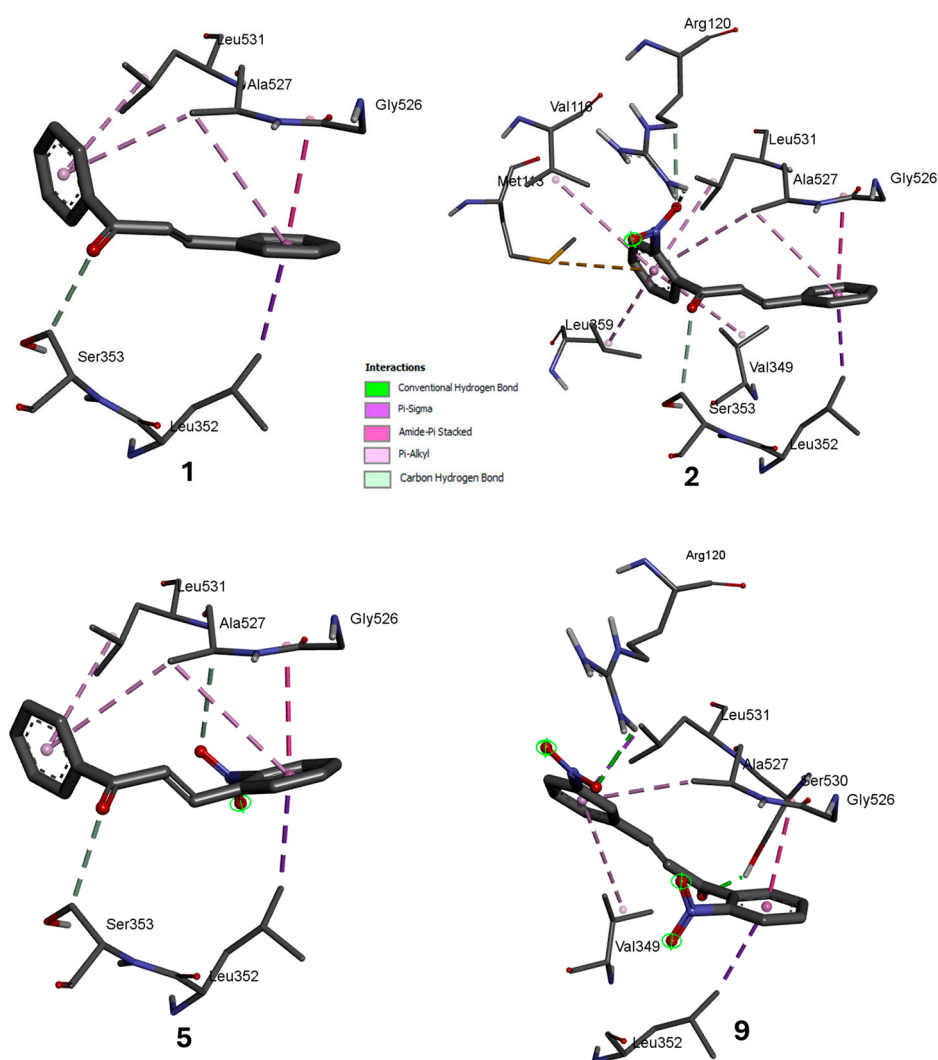
Figure 5. Docking of nitrochalcones **1**, **2**, **5**, and **9** with the COX-1 enzyme.

The coupling of the chalcone and nitro group-containing chalcones at the COX-1 binding site with CEL allowed the identification of a generic binding mode for chalcone rings A and B (Figure 6A). The residues anchoring the rings were primarily Ala[527], which interacted with both rings of compounds **1**, **2**, **5**, and **9**. Leu[352], Leu[531], and Leu[359] were subsequently identified as contributing to stabilizing the chalcone core (Figure 6B). The

orientations of compounds **1**, **2**, and **5** bound to COX-1 were identical, whereas compound **9** could reverse the rings' position (Figure 6C). The carbonyl-like structural fragment was observed to contribute to the formation of a hydrogen bond both when oriented toward Ser[353] (compounds **1**, **2**, and **5**) and when oriented toward Ser[530] (compound **9**) (Figure 6B,C).
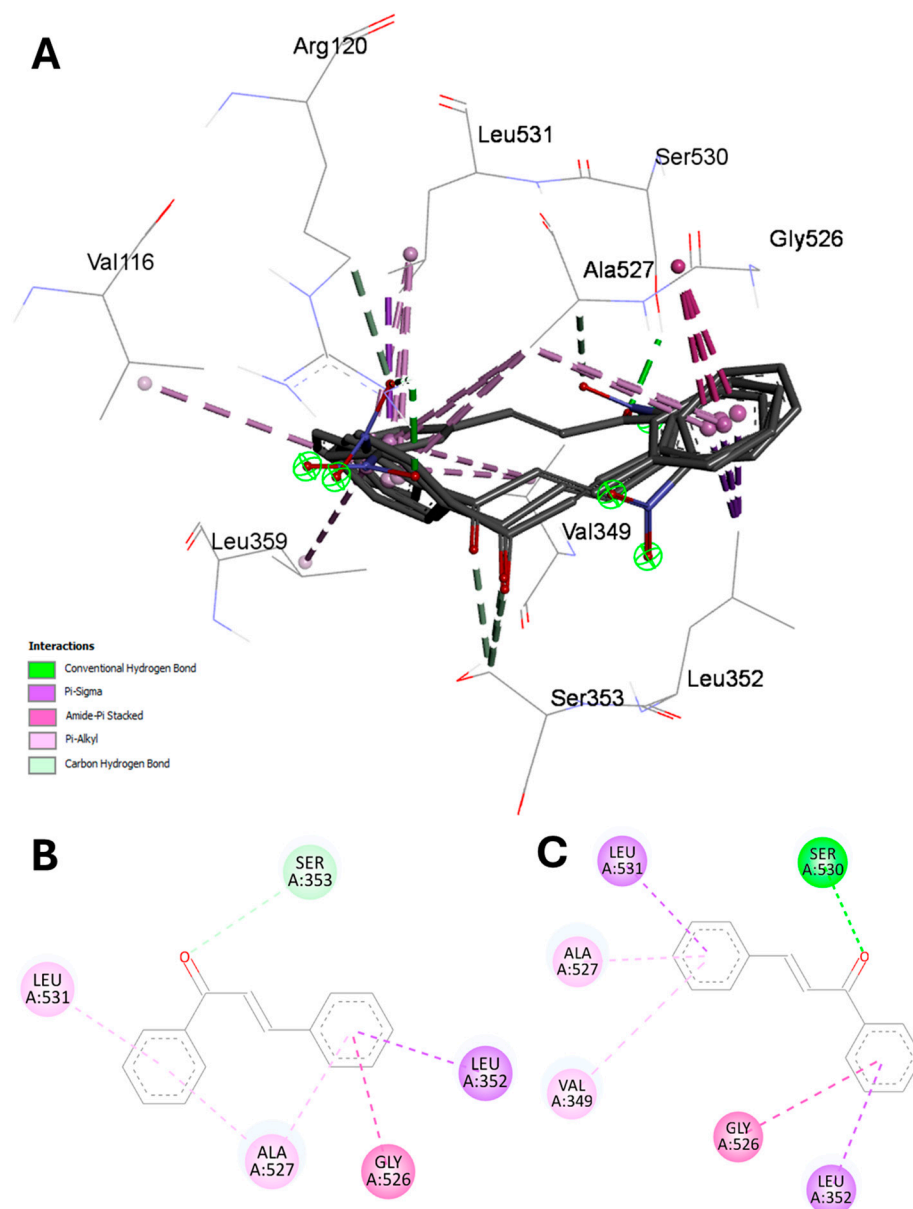

Figure 6. Overlayed poses were obtained for compounds **1**, **2**, **5**, and **9** with the chalcone's ring-stabilizing residues A and B (**A**). The base structure of the chalcone interacts with the residues, stabilizing the chalcone base skeleton (**B**,**C**).

3.3.2. Cyclooxygenase-2

Molecular docking studies of compounds **1**, **2**, **5**, and **9** with the COX-2 enzyme revealed affinity energies ranging from −9.3 to −8.2 kcal/mol, indicating compound-specific interactions. All the compounds except **9** exhibited carbonyl group interactions with Ser[339] via carbon–hydrogen bonding. In ring A, compounds **1** and **2** formed π–alkyl bonds with Val[102], whereas compounds **5** and **9** exhibited similar interactions with Val[509]. The A and B rings of compounds **1** and **2** interacted with Ala[513] via π–alkyl bonds, whereas in compounds **5** and **9**, only ring B had similar interactions with Ala[513]. Compound **1**

exhibited additional interactions, including a π–π T-shaped interaction between ring A and Tyr[341], a stacked amide–π interaction between ring B and the amino acid Gly[512], and a π–π-stack interaction between ring B and Phe[504]. In the case of compound **2**, ring A did not exhibit any additional interactions. However, the nitro group present in the ortho position of this same ring engaged in conventional hydrogen bonding with Arg[106], whereas ring B demonstrated interactions with Gly[512] and Phe[504] through stacked amide–π interactions. In the case of compound **5**, ring A also interacted with Leu[338] via a π–alkyl bond, whereas ring B, which contains a nitro group in the ortho position, interacted with Tyr[341] via a π–π T-shaped interaction. Additionally, one of the oxygens of the nitro group interacted with Arg[106] via a conventional hydrogen bond.

In compound **9**, ring A, which contains one of the two nitro groups in the ortho position, interacts with Leu[338] via a π–alkyl bond and with Trp[373] via a π–π T-shaped interaction. Ring B, which contains the nitro group in the meta position, interacts with Leu[517] via a π–alkyl bond. However, the ring's nitro groups do not interact with any amino acids. These observations underscore the impact of varying positions and substitutions of compounds on the affinity and interaction pattern with active COX-2 residues, offering a comprehensive understanding of the binding mechanisms at the molecular level (Figure 7).
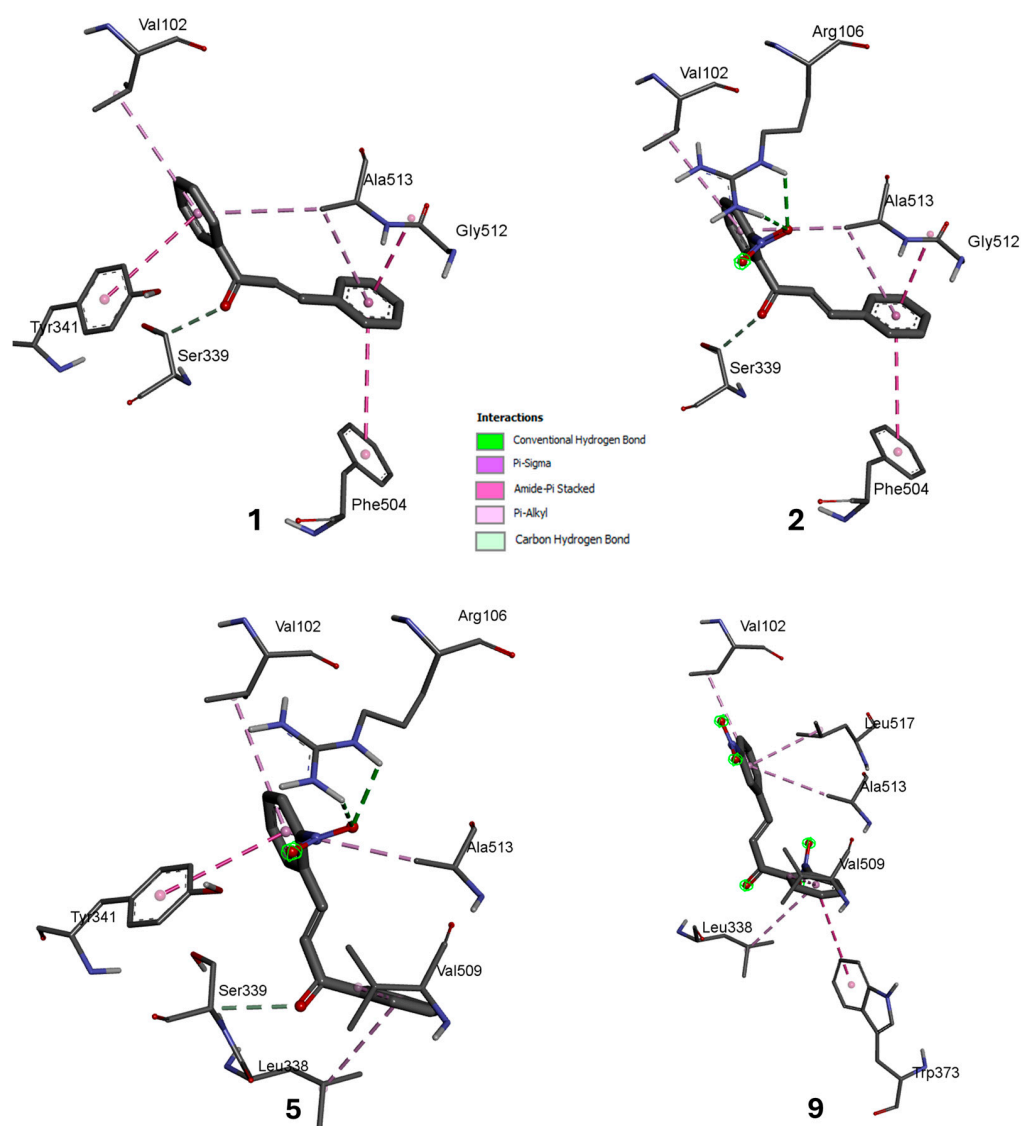
Figure 7. Docking of nitrochalcones **1**, **2**, **5**, and **9** with the COX-2 enzyme.

The docking of the chalcone and nitrochalcones at the COX-2 binding site with CEL enabled identifying a generic binding mode for the chalcone rings A and B (Figure 8A). The residues responsible for stabilizing the rings were primarily Ala[513], which interacted with both rings of compounds **1**, **2**, **5**, and **9**. Val[102], Tyr[341], Phe[504], and Gly[512] were subsequently identified as contributing to stabilizing the chalcone core (Figure 8B). All the compounds exhibited the same carbonyl orientation when bound to COX-2. However, for compounds **1** and **2**, the rings could be reversed in position, although this did not affect the hydrogen bond interaction with Ser[339].
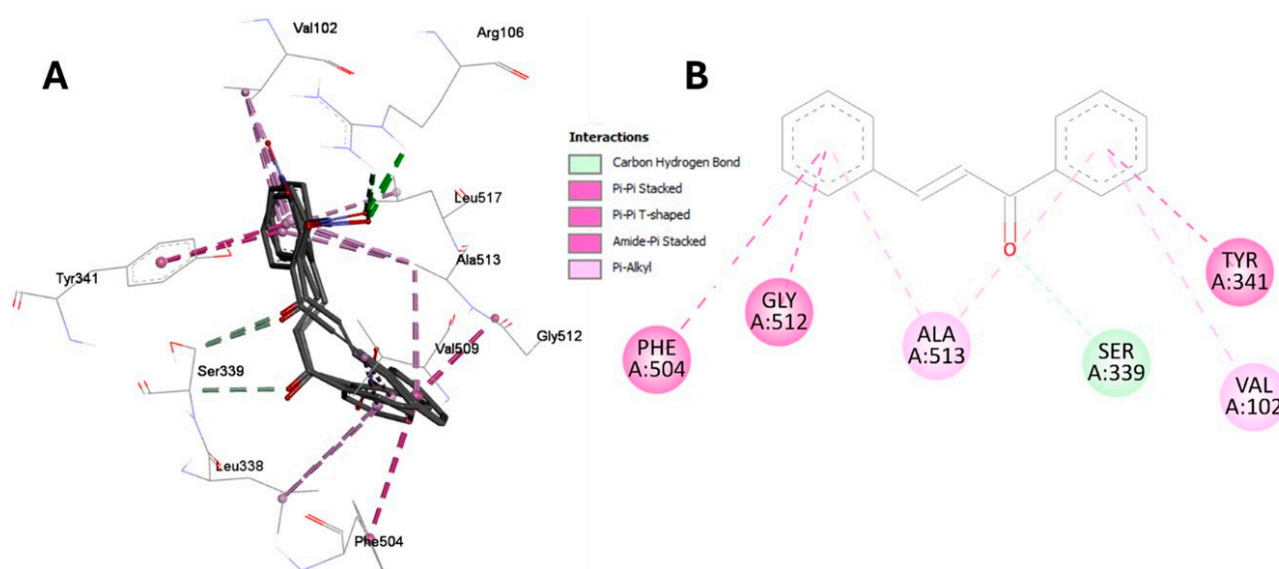
Figure 8. Overlayed poses were obtained for compounds **1**, **2**, **5**, and **9** with the residues stabilizing the chalcone's A and B rings (**A**). The structure of the base chalcone interacts with the residues, stabilizing the chalcone base skeleton (**B**).

The COX-2 coupling results demonstrated that introducing a nitro group to ring A of the chalcone enabled the establishment of a hydrogen bond with Arg[106].

Given the results observed between COX-1 and COX-2 and the high degree of structural resemblance between the two COX isoforms, a sequence alignment was conducted. The resulting data indicated an identity percentage of 61.4% and a high similarity percentage of 80.1%.

The calculated selectivity index revealed that compound **2** has greater selectivity for COX-2 (Table 2). However, the potency of the control CEL was 3.7-fold more significant than that of compound **2** and **Indo**, which are known to inhibit both COX-1 and COX-2. These findings suggest that the selectivity index of compound **2** may not be a reliable indicator of its selective profile.

Table 2. Molecular docking results and selectivity analysis of the chalcones with the highest activity.

	COX-1		COX-2		
	Affinity (Kcal/mol)	K_i * (E^{-7}) #	Affinity (Kcal/mol)	K_i (E^{-7}) #	SI **
1	−7.8 ± 0	19.1 ± 0	−8.2 ± 0.10	9.8 ± 1.70	1.95
2	−7.5 ± 0	31.8 ± 0	−9.1 ± 0.03	2.17 ± 0.11	14.64
5	−8.0 ± 0	13.6 ± 0	−8.99 ± 0.15	2.6 ± 0.25	5.25
9	−8.0 ± 0	13.6 ± 0	−9.3 ± 0.05	1.5 ± 0	8.97
Indo	−5.0 ± 0.05	2078.6 ± 151.9	−6.8 ± 0.413	142.4 ± 265.17	14.59
CEL	−6.1 ± 0.23	344.7 ± 227.6	−8.45 ± 0.05	6.3 ± 0.55	54.02

Data in the table report the mean ± standard deviation. * Ki: inhibition constant. # Values are in exponent factors (−7). ** SI: selectivity index.

3.3.3. Endothelial Nitric Oxide Synthase

In the molecular docking study of compounds **1** and **7** with the eNOS enzyme, an affinity energy of -6.5 kcal/mol was obtained for both compounds. The experiments demonstrated that both compounds engage in hydrogen bonding with the amino acid Arg[365] through their carbonyl groups. Ring A of both compounds interacted with the amino acid Pro[451] via a π–alkyl bond and a Hem[500] group. In the case of compound **1**, the interaction occurred via a stacked π–π bond, whereas in the case of compound **7**, it occurred via a π–sigma bond. While ring B exhibited an interaction only with Ala[446], in compound **1**, this interaction was conducted through a π–sigma bond, and in compound **7**, it occurred through a π–alkyl bond. Concerning compound **7**, which contains a nitro group in the B-ring, no interaction of the nitro group with any amino acid was observed. The primary distinction between these compounds is evident in compound **1**, which has an additional interaction of the double bond with the amino acid Trp[447] (Figure 9).
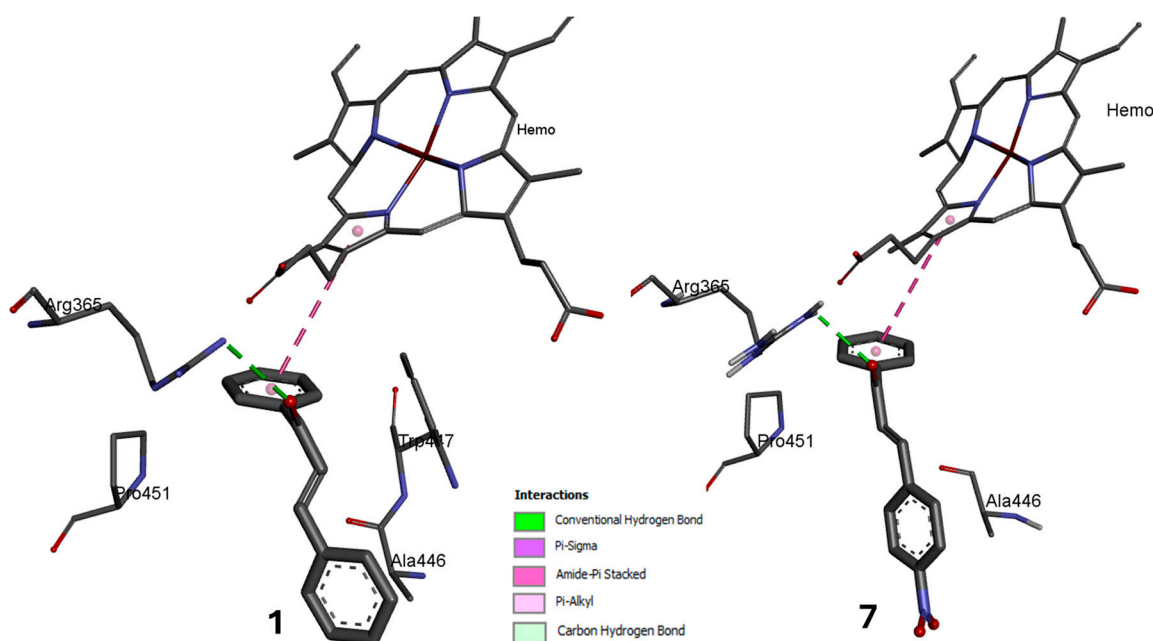
Figure 9. Docking of nitrochalcones **1** and **7** with the eNOS enzyme.

4. Discussion

The increasing interest in exploring the various medicinal properties of nitro group-containing compounds [49] has led to investigations of the anti-inflammatory and vasorelaxant activities of chalcones with a nitro group at different positions of the molecule. The findings of the present study indicate that nitro group-containing chalcones have evident anti-inflammatory and vasorelaxant effects.

The anti-inflammatory activity of the chalcones evaluated in this study demonstrated that compound **1**, a chalcone devoid of substituents, exhibited a diminished level of potency relative to nitrochalcones **2**, **4**, **5**, and **6**, which contain a nitro group. Conversely, compounds **3**, **8**, and **10** demonstrated a reduced potency compared with that of compound **1**. Compared with the reference drug **Indo**, compounds **2** and **5** demonstrated equivalent or greater potency at the same dose evaluated. This finding indicates that the incorporation of the nitro group into specific positions within the chalcone structure can markedly increase its anti-inflammatory potency, potentially attaining levels greater than those of a reference drug.

Nitro group-containing chalcones **2** and **5**, which feature a nitro group at the ortho position on both the A and B rings, demonstrated the most pronounced anti-inflammatory effects. This finding aligns with a previous study conducted by our research group. In the aforementioned study, the anti-inflammatory effect of nitrochalcones in a model of

plantar edema induced by carrageenan was reported. The chalcone with the nitro group in the ortho position in the A ring was identified as the most effective isomer among those studied [34]. These findings have been corroborated by other research groups who have conducted anti-inflammatory assessments of select chalcone derivatives with a nitro group. These results indicate that compounds with a nitro group at the *ortho* position exhibit the highest anti-inflammatory activity [50,51].

The anti-inflammatory activity of chalcones has been attributed primarily to the enone present in the structure of the compound [52], which has been demonstrated to be essential for blocking the degranulation of mast cells in the anti-inflammatory process. Consequently, it can be postulated that the enone present, together with the nitro group in the molecular structure, can generate a series of electronic effects, thereby contributing to significant anti-inflammatory activity. In this study, a correlation between the ortho position of the nitro group in chalcones and their anti-inflammatory activity is observed. Chemically, the nitro group in the ortho position introduces a strong resonance effect and electron delocalization which increases the polarization of the enone system, which may possibly enhance the reactivity of the molecule against enzymes involved in inflammatory processes [53].

To our knowledge, the anti-inflammatory effect of chalcones with two nitro groups has not been discussed in the literature. Therefore, the results obtained represent a challenging approach to chalcones with two nitro groups in their structure and it will be necessary to conduct further investigation about their possible interactions with pharmacological targets.

Many studies have proposed a mechanism of action for the anti-inflammatory activity of chalcones, which is thought to involve the inhibition of cyclooxygenases (COXs) [54–56]. In this study, molecular docking calculations were conducted with COX-1 and COX-2. The results demonstrated that compound **2** had the greatest number of interactions with COX-1, whereas compound **5** had the greatest number of interactions with COX-2. These findings align with the experimental data, which indicated that both compounds **2** and **5** exhibited the greatest anti-inflammatory potency.

From an electronic point of view, docking simulations confirm that the nitro group at the ortho position of the A-ring of chalcones establishes crucial hydrogen bonds with key residues in COX-1 and COX-2 enzymes, such as Arg^{120} in COX-1 and Arg^{106} in COX-2. These interactions confirm the affinity of the nitro groups of the chalcones for the active sites of both COX isoforms, resulting in enhanced inhibition of inflammatory activity [57].

Conversely, the nitro group of chalcones has the capacity to donate NO and facilitate a vasorelaxant effect [58]. This research represents the first report of the vasorelaxant effects of the studied compounds (**1–10**). Notably, chalcones bearing nitro groups at different positions showed similar or lower vasorelaxant effects than compound 1 (which lacked a nitro group). Since the most active compounds were **1** and **7**, their mechanism of action was investigated. The reduction in the vasorelaxant effect of chalcones 1 and 7 in the presence of L-NAME suggests the involvement of the NO pathway in the pharmacological effect.

This is the reason why, in Table 1, chalcones have a greater effect with endothelium than without endothelium, and Figure 4 was constructed only in the presence of endothelium.

These findings are corroborated by the results of molecular docking, which indicate that compounds **1** and **7** interact with the eNOS enzyme via specific interactions. However, the vasorelaxant effect of compound **7** was diminished when **Indo** or atropine was included in the experiments. These findings make compound **7** a promising subject for further study, as it likely has dual vasorelaxant mechanisms, whereby more than one endothelial cell-dependent vasorelaxant pathway is involved, such as the inhibition of prostaglandin production or the activation of muscarinic receptors [59,60].

5. Conclusions

The present study aimed to assess the anti-inflammatory and vasorelaxant properties of a series of chalcones with nitro groups at different positions. Compounds **2**, **5**, and **9**, with the nitro group in the ortho position, demonstrated the highest percentage of inhibition of inflammation and exhibited the most significant interactions in molecular docking studies

with COX-2. Furthermore, the presence of the nitro group in the B-ring in the para position of compound **7** was found to enhance its vasorelaxant effect, primarily through the NO pathway. This is likely due to the interaction of the nitro group with eNOS. These results demonstrate that the nitro group and its position within the chalcone structure play pivotal roles in influencing its anti-inflammatory and vasorelaxant activities.

Author Contributions: Writing—original draft, A.Y.H.; writing—review & editing, C.E.L.-G.; writing—original draft, supervision, and project administration, A.G.-R.; methodology, formal analysis and conceptualization, O.H.-A.; methodology and visualization, O.A.P.-M.; investigation and conceptualization, N.R.-C.; methodology and investigation, M.H.-R.; writing—review & editing, formal analysis, and visualization, M.Á.V.-R.; methodology, A.J.G.-G.; formal analysis and conceptualization, E.J.M.-S.; methodology, R.V.-C. All authors have read and agreed to the published version of the manuscript.

Institutional Review Board Statement: The Local Health and Ethics Research Committee of the Instituto Mexicano del Seguro Social (IMSS) approved the present project with registration R-2020-1702-008, and the Institutional Commission on Research Ethics of the División Académica de Ciencias de la Salud (UJAT) approved the present project with registration CIEI-UJAT-0927.

Informed Consent Statement: Not applicable.

Data Availability Statement: The data presented in the study are available in the article.

Conflicts of Interest: The authors state that they have no financial interests or personal relationships that could have influenced the research presented in this paper.

References

1. Bennett, J.M.; Reeves, G.; Billman, G.E.; Sturmberg, J.P. Inflammation–Nature's Way to Efficiently Respond to All Types of Challenges: Implications for Understanding and Managing "the Epidemic" of Chronic Diseases. *Front. Med.* **2018**, *5*, 316. [CrossRef] [PubMed]
2. Furman, D.; Campisi, J.; Verdin, E.; Carrera-Bastos, P.; Targ, S.; Franceschi, C.; Ferrucci, L.; Gilroy, D.W.; Fasano, A.; Miller, G.W. Chronic Inflammation in the Etiology of Disease across the Life Span. *Nat. Med.* **2019**, *25*, 1822–1832. [CrossRef] [PubMed]
3. He, Y.; Yue, Y.; Zheng, X.; Zhang, K.; Chen, S.; Du, Z. Curcumin, Inflammation, and Chronic Diseases: How Are They Linked? *Molecules* **2015**, *20*, 9183–9213. [CrossRef]
4. Ho, K.Y.; Gwee, K.A.; Cheng, Y.K.; Yoon, K.H.; Hee, H.T.; Omar, A.R. Nonsteroidal Anti-Inflammatory Drugs in Chronic Pain: Implications of New Data for Clinical Practice. *J. Pain Res.* **2018**, *11*, 1937–1948. [CrossRef]
5. Bindu, S.; Mazumder, S.; Bandyopadhyay, U. Non-Steroidal Anti-Inflammatory Drugs (NSAIDs) and Organ Damage: A Current Perspective. *Biochem. Pharmacol.* **2020**, *180*, 114147. [CrossRef] [PubMed]
6. Sales, T.A.; Marcussi, S.; Ramalho, T.C. Current Anti-Inflammatory Therapies and the Potential of Secretory Phospholipase A2 Inhibitors in the Design of New Anti-Inflammatory Drugs: A Review of 2012–2018. *Curr. Med. Chem.* **2020**, *27*, 477–497. [CrossRef]
7. Alsina-Sánchez, Á.M.; Montalvo-Vázquez, S.; Grafals-Ruiz, N.; Acosta, C.; Ormé, E.M.; Rodríguez, I.; Delgado-Rivera, S.M.; Tinoco, A.D.; Dharmawardhane, S.; Montes-González, I.C. Synthesis of Novel Heterocyclic Ferrocenyl Chalcones and Their Biological Evaluation. *ACS Omega* **2023**, *8*, 34377–34387. [CrossRef]
8. Pérez-González, A.; Castañeda-Arriaga, R.; Guzmán-López, E.G.; Hernández-Ayala, L.F.; Galano, A. Chalcone Derivatives with a High Potential as Multifunctional Antioxidant Neuroprotectors. *ACS Omega* **2022**, *7*, 38254–38268. [CrossRef]
9. Elkanzi, N.A.A.; Hrichi, H.; Alolayan, R.A.; Derafa, W.; Zahou, F.M.; Bakr, R.B. Synthesis of Chalcones Derivatives and Their Biological Activities: A Review. *ACS Omega* **2022**, *7*, 27769–27786. [CrossRef]
10. Constantinescu, T.; Mihis, A.G. Two Important Anticancer Mechanisms of Natural and Synthetic Chalcones. *Int. J. Mol. Sci.* **2022**, *23*, 11595. [CrossRef]
11. Hernández-Rivera, J.L.; Espinoza-Hicks, J.C.; Chacon-Vargas, K.F.; Carrillo-Campos, J.; Sánchez-Torres, L.E.; Camacho-Davila, A.A. Synthesis, Characterization and Evaluation of Prenylated Chalcones Ethers as Promising Antileishmanial Compounds. *Mol. Divers.* **2023**, *27*, 2073–2092. [CrossRef] [PubMed]
12. Lai, W.; Chen, J.; Gao, X.; Jin, X.; Chen, G.; Ye, L. Design and Synthesis of Novel Chalcone Derivatives: Anti-Breast Cancer Activity Evaluation and Docking Study. *Int. J. Mol. Sci.* **2023**, *24*, 15549. [CrossRef] [PubMed]
13. Goyal, K.; Kaur, R.; Goyal, A.; Awasthi, R. Chalcones: A Review on Synthesis and Pharmacological Activities. *J. Appl. Pharm. Sci.* **2021**, *11*, 1–14.

14. Jasim, H.A.; Nahar, L.; Jasim, M.A.; Moore, S.A.; Ritchie, K.J.; Sarker, S.D. Chalcones: Synthetic Chemistry Follows Where Nature Leads. *Biomolecules* **2021**, *11*, 1203. [CrossRef]

15. Higgs, J.; Wasowski, C.; Marcos, A.; Jukič, M.; Paván, C.H.; Gobec, S.; de Tezanos Pinto, F.; Colettis, N.; Marder, M. Chalcone Derivatives: Synthesis, in Vitro and in Vivo Evaluation of Their Anti-Anxiety, Anti-Depression and Analgesic Effects. *Heliyon* **2019**, *5*, e01376. [CrossRef]

16. Burmaoglu, S.; Algul, O.; Gobek, A.; Aktas Anil, D.; Ulger, M.; Erturk, B.G.; Kaplan, E.; Dogen, A.; Aslan, G. Design of Potent Fluoro-Substituted Chalcones as Antimicrobial Agents. *J. Enzym. Inhib. Med. Chem.* **2017**, *32*, 490–495. [CrossRef]

17. Jiang, Y.; Yang, Q.; Zhang, S. Computation of Structure Activity and Design of Chalcone Derivatives. *Comput. Chem.* **2019**, *7*, 51. [CrossRef]

18. Nawaz, T.; Tajammal, A.; Qurashi, A.W. Chalcones As Broad-Spectrum Antimicrobial Agents: A Comprehensive Review And Analysis Of Their Antimicrobial Activities. *ChemistrySelect* **2023**, *8*, e202302798. [CrossRef]

19. Rajendran, G.; Bhanu, D.; Aruchamy, B.; Ramani, P.; Pandurangan, N.; Bobba, K.N.; Oh, E.J.; Chung, H.Y.; Gangadaran, P.; Ahn, B.-C. Chalcone: A Promising Bioactive Scaffold in Medicinal Chemistry. *Pharmaceuticals* **2022**, *15*, 1250. [CrossRef]

20. Dos Santos, A.T.L.; de Araújo-Neto, J.B.; da Silva, M.M.C.; da Silva, M.E.P.; Carneiro, J.N.P.; Fonseca, V.J.A.; Coutinho, H.D.M.; Bandeira, P.N.; Dos Santos, H.S.; da Silva Mendes, F.R. Synthesis of Chalcones and Their Antimicrobial and Drug Potentiating Activities. *Microb. Pathog.* **2023**, *180*, 106129. [CrossRef]

21. Mahapatra, D.K.; Bharti, S.K.; Asati, V. Chalcone Derivatives: Anti-Inflammatory Potential and Molecular Targets Perspectives. *Curr. Top. Med. Chem.* **2017**, *17*, 3146–3169. [CrossRef] [PubMed]

22. Yuan, G.; Wahlqvist, M.L.; He, G.; Yang, M.; Li, D. Natural Products and Anti-Inflammatory Activity. *Asia Pac. J. Clin. Nutr.* **2006**, *15*, 127–286.

23. Krishnamoorthy, S.; Honn, K. V Inflammation and Disease Progression. *Cancer Metastasis Rev.* **2006**, *25*, 481–491. [CrossRef] [PubMed]

24. Selçuk, K.T. Epidemiology of Inflammation-Related Diseases. In *Role of Nutrition in Providing Pro-/Anti-Inflammatory Balance: Emerging Research and Opportunities*; IGI Global: Hershey, PA, USA, 2020; pp. 24–44.

25. Legeay, S.; Trân, K.; Abatuci, Y.; Faure, S.; Helesbeux, J.-J. Novel Insights into the Mode of Action of Vasorelaxant Synthetic Polyoxygenated Chalcones. *Int. J. Mol. Sci.* **2020**, *21*, 1609. [CrossRef]

26. da Silva, G.M.; da Silva, M.C.; Nascimento, D.V.G.; Lima Silva, E.M.; Gouvêa, F.F.F.; de França Lopes, L.G.; Araújo, A.V.; Ferraz Pereira, K.N.; de Queiroz, T.M. Nitric Oxide as a Central Molecule in Hypertension: Focus on the Vasorelaxant Activity of New Nitric Oxide Donors. *Biology* **2021**, *10*, 1041. [CrossRef]

27. Sherikar, A.S.; Bhatia, M.S.; Dhavale, R.P. Identification and Investigation of Chalcone Derivatives as Calcium Channel Blockers: Pharmacophore Modeling, Docking Studies, In Vitro Screening, and 3D-QSAR Analysis. *Curr. Comput.-Aided Drug Des.* **2021**, *17*, 676–686. [CrossRef]

28. Li, J.; Li, D.; Xu, Y.; Guo, Z.; Liu, X.; Yang, H.; Wu, L.; Wang, L. Design, Synthesis, Biological Evaluation, and Molecular Docking of Chalcone Derivatives as Anti-Inflammatory Agents. *Bioorg. Med. Chem. Lett.* **2017**, *27*, 602–606. [CrossRef]

29. Bastrakov, M.; Starosotnikov, A. Recent Progress in the Synthesis of Drugs and Bioactive Molecules Incorporating Nitro (Het) Arene Core. *Pharmaceuticals* **2022**, *15*, 705. [CrossRef] [PubMed]

30. Lochmann, C.; Luxford, T.F.M.; Makurat, S.; Pysanenko, A.; Kočišek, J.; Rak, J.; Denifl, S. Low-Energy Electron Induced Reactions in Metronidazole at Different Solvation Conditions. *Pharmaceuticals* **2022**, *15*, 701. [CrossRef] [PubMed]

31. Erlanson, D.A.; Fesik, S.W.; Hubbard, R.E.; Jahnke, W.; Jhoti, H. Twenty Years on: The Impact of Fragments on Drug Discovery. *Nat. Rev. Drug Discov.* **2016**, *15*, 605–619. [CrossRef]

32. Noriega, S.; Cardoso-Ortiz, J.; López-Luna, A.; Cuevas-Flores, M.D.R.; Flores De La Torre, J.A. The Diverse Biological Activity of Recently Synthesized Nitro Compounds. *Pharmaceuticals* **2022**, *15*, 717. [CrossRef] [PubMed]

33. Torres-Sauret, Q.; Sánchez, C.A.; de la Fuente, L.F.R.; Montero, P.P.; Dorante, M.T.F.; del Carmen Méndez-Moreno, J.; Reyes, M.Á.V.; Mendoza-Lorenzo, P. Síntesis de (E)-1, 3-Difenil-Prop-2-En-1-Ona y Su Evaluación Sobre El Crecimiento de Una Cepa de S. Aureus Fármacorresistente. *Rev. Mex. De Cienc. Farm.* **2017**, *48*, 67–74.

34. Gómez-Rivera, A.; Aguilar-Mariscal, H.; Romero-Ceronio, N.; Roa-de la Fuente, L.F.; Lobato-García, C.E. Synthesis and Anti-Inflammatory Activity of Three Nitro Chalcones. *Bioorg. Med. Chem. Lett.* **2013**, *23*, 5519–5522. [CrossRef] [PubMed]

35. Matus, E.A. *Síntesis y Exploración de La Adición Tipo Michael En Enonas y Determinación de La Actividad Antiinflamatorias de Nitrochalconas*; Universidad Juárez Autónoma de Tabasco: Villahermosa, Mexico, 2014.

36. Hidalgo, A.Y.; Velasco, M.; Sánchez-Lara, E.; Gómez-Rivera, A.; Vilchis-Reyes, M.A.; Alvarado, C.; Herrera-Ruiz, M.; López-Rodríguez, R.; Romero-Ceronio, N.; Lobato-García, C.E. Synthesis, Crystal Structures, and Molecular Properties of Three Nitro-Substituted Chalcones. *Crystals* **2021**, *11*, 1589. [CrossRef]

37. de la Federación, D.O. Norma Oficial Mexicana NOM-062-ZOO-1999, Especificaciones Técnicas Para La Producción, Cuidado y Uso de Los Animales de Laboratorio. *D. Of. La Fed.* **2001**, *477*.

38. Zimmermann, M. Ethical Guidelines for Investigations of Experimental Pain in Conscious Animals. *Pain* **1983**, *16*, 109–110. [CrossRef]

39. Payá, M.; Ferrándiz, M.L.; Sanz, M.J.; Bustos, G.; Blasco, R.; Rios, J.L.; Alcaraz, M.J. Study of the Antioedema Activity of Some Seaweed and Sponge Extracts from the Mediterranean Coast in Mice. *Phytother. Res.* **1993**, *7*, 159–162. [CrossRef]

40. Rodríguez-Morales, S.; Ocampo-Medina, B.; Romero-Ceronio, N.; Alvarado-Sánchez, C.; Vilchis-Reyes, M.Á.; Roa de la Fuente, L.F.; Ortiz-Andrade, R.; Hernández-Abreu, O. Metabolic Profiling of Vasorelaxant Extract from *Malvaviscus arboreus* by LC/QTOF-MS. *Chem. Biodivers.* **2021**, *18*, e2000820. [CrossRef]

41. Hernández-Abreu, O.; Castillo-España, P.; León-Rivera, I.; Ibarra-Barajas, M.; Villalobos-Molina, R.; González-Christen, J.; Vergara-Galicia, J.; Estrada-Soto, S. Antihypertensive and Vasorelaxant Effects of Tilianin Isolated from Agastache Mexicana Are Mediated by NO/CGMP Pathway and Potassium Channel Opening. *Biochem. Pharmacol.* **2009**, *78*, 54–61. [CrossRef]

42. Rimon, G.; Sidhu, R.S.; Lauver, D.A.; Lee, J.Y.; Sharma, N.P.; Yuan, C.; Frieler, R.A.; Trievel, R.C.; Lucchesi, B.R.; Smith, W.L. Coxibs Interfere with the Action of Aspirin by Binding Tightly to One Monomer of Cyclooxygenase-1. *Proc. Natl. Acad. Sci. USA* **2010**, *107*, 28–33. [CrossRef]

43. Wang, J.L.; Limburg, D.; Graneto, M.J.; Springer, J.; Hamper, J.R.B.; Liao, S.; Pawlitz, J.L.; Kurumbail, R.G.; Maziasz, T.; Talley, J.J. The Novel Benzopyran Class of Selective Cyclooxygenase-2 Inhibitors. Part 2: The Second Clinical Candidate Having a Shorter and Favorable Human Half-Life. *Bioorganic Med. Chem. Lett.* **2010**, *20*, 7159–7163. [CrossRef] [PubMed]

44. Li, H.; Jamal, J.; Plaza, C.; Pineda, S.H.; Chreifi, G.; Jing, Q.; Cinelli, M.A.; Silverman, R.B.; Poulos, T.L. Structures of Human Constitutive Nitric Oxide Synthases. *Acta Crystallogr. Sect. D Biol. Crystallogr.* **2014**, *70*, 2667–2674. [CrossRef] [PubMed]

45. Hanwell, M.D.; Curtis, D.E.; Lonie, D.C.; Vandermeersch, T.; Zurek, E.; Hutchison, G.R. Avogadro: An Advanced Semantic Chemical Editor, Visualization, and Analysis Platform. *J. Cheminformatics* **2012**, *4*, 17. [CrossRef] [PubMed]

46. Morris, G.M.; Huey, R.; Lindstrom, W.; Sanner, M.F.; Belew, R.K.; Goodsell, D.S.; Olson, A.J. AutoDock4 and AutoDockTools4: Automated Docking with Selective Receptor Flexibility. *J. Comput. Chem.* **2009**, *30*, 2785–2791. [CrossRef] [PubMed]

47. Trott, O.; Olson, A.J. AutoDock Vina: Improving the Speed and Accuracy of Docking with a New Scoring Function, Efficient Optimization, and Multithreading. *J. Comput. Chem.* **2010**, *31*, 455–461. [CrossRef]

48. BIOVIA Discovery Studio. *Discovery Studio Modeling Environment*; Dassault Systemes, Release; BIOVIA Discovery Studio: San Diego, CA, USA, 2015; Volume 4, p. 2016.

49. Szatylowicz, H.; Jezuita, A.; Ejsmont, K.; Krygowski, T.M. Classical and Reverse Substituent Effects in Meta-and Para-Substituted Nitrobenzene Derivatives. *Struct. Chem.* **2017**, *28*, 1125–1132. [CrossRef]

50. Bano, S.; Javed, K.; Ahmad, S.; Rathish, I.G.; Singh, S.; Chaitanya, M.; Arunasree, K.M.; Alam, M.S. Synthesis of Some Novel Chalcones, Flavanones and Flavones and Evaluation of Their Anti-Inflammatory Activity. *Eur. J. Med. Chem.* **2013**, *65*, 51–59. [CrossRef]

51. Bukhari, S.N.A.; Ahmad, W.; Butt, A.M.; Ahmad, N.; Amjad, M.W.B.; Hussain, M.A.; Shah, V.H.; Trivedi, A.R. Synthesis and Evaluation of Chalcone Analogues and Pyrimidines as Cyclooxygenase (COX) Inhibitors. *Afr. J. Pharm. Pharmacol.* **2012**, *6*, 1064–1068.

52. Hsieh, H.; Tsao, L.; Wang, J.; Lin, C. Synthesis and Anti-inflammatory Effect of Chalcones. *J. Pharm. Pharmacol.* **2000**, *52*, 163–171. [CrossRef] [PubMed]

53. Yadav, A.; Sharma, V.; Singh, G. Anti-Inflammatory Potential of Chalcone Related Compounds: An Updated Review. *ChemistrySelect* **2024**, *9*, e202401321. [CrossRef]

54. Jantan, I.; Bukhari, S.N.A.; Adekoya, O.A.; Sylte, I. Studies of Synthetic Chalcone Derivatives as Potential Inhibitors of Secretory Phospholipase A2, Cyclooxygenases, Lipoxygenase and pro-Inflammatory Cytokines. *Drug Des. Dev. Ther.* **2014**, *8*, 1405–1418. [CrossRef] [PubMed]

55. Araico, A.; Terencio, M.C.; Alcaraz, M.J.; Dominguez, J.N.; Leon, C.; Ferrandiz, M.L. Phenylsulphonyl Urenyl Chalcone Derivatives as Dual Inhibitors of Cyclo-Oxygenase-2 and 5-Lipoxygenase. *Life Sci.* **2006**, *78*, 2911–2918. [CrossRef]

56. ur Rashid, H.; Xu, Y.; Ahmad, N.; Muhammad, Y.; Wang, L. Promising Anti-Inflammatory Effects of Chalcones via Inhibition of Cyclooxygenase, Prostaglandin E2, Inducible NO Synthase and Nuclear Factor Kb Activities. *Bioorg. Chem.* **2019**, *87*, 335–365. [CrossRef] [PubMed]

57. Siddiqa, A.; Tajammal, A.; Irfan, A.; Azam, M.; Munawar, M.A.; Hardy, R.S.; Basra, M.A.R. Synthesis, Molecular Docking, Bio-Evaluation and Quantitative Structure Activity Relationship of New Chalcone Derivatives as Antioxidants. *J. Mol. Struct.* **2023**, *1277*, 134814. [CrossRef]

58. Sherikar, A.; Dhavale, R.; Bhatia, M. Investigation of Anti-inflammatory, Nitric Oxide Donating, Vasorelaxation and Ulcerogenic Activities of 1, 3-diphenylprop-2-en-1-one Derivatives in Animal Models. *Clin. Exp. Pharmacol. Physiol.* **2019**, *46*, 483–495. [CrossRef]

59. Whittle, B.J.R. Temporal Relationship between Cyclooxygenase Inhibition, as Measured by Prostacyclin Biosynthesis, and the Gastrointestinal Damage Induced by Indomethacin in the Rat. *Gastroenterology* **1981**, *80*, 94–98. [CrossRef]

60. Choi, Y.D.; Chung, W.S.; Choi, H.K. The Action Mechanism of Relaxation Effect of Atropine on the Isolated Rabbit Corpus Cavernosum. *J. Urol.* **1999**, *161*, 1976–1979. [CrossRef]